Volcanic eruptions following M ≥ 9 megathrust earthquakes: Implications for the Sumatra-Andaman volcanoes

Thomas R. Walter
GeoForschungsZentrum (GFZ), Telegrafenberg, D-14473, Potsdam, Germany
Falk Amelung
Department of Marine Geology and Geophysics, Rosenstiel School of Marine and Atmospheric Sciences, University of Miami, Miami, Florida 33149, USA

ABSTRACT

Two volcanic eruptions in the Sumatra-Andaman arc that followed the disastrous M 9.3 earthquake of 26 December 2004 raise the question of whether these eruptions were triggered by the earthquake. Here we present new evidence to suggest that earthquake-induced decompression of the volcano magma systems leads to such eruptions. Numerical modeling reveals that other megathrust earthquakes induced volumetric expansion in the areas where volcanoes erupted. We suggest that abrupt decompression of a magma reservoir and/or its feeding system initiates processes that increase magma overpressure, and can ultimately lead to an eruption. Our evaluation of earthquake-induced deformation fields indicates which specific volcanoes are brought closer to eruption by earthquake rupture. Our analysis can provide important information for future volcanic risk evaluation in areas with regional fault systems prone to large magnitude earthquakes.

Keywords: volcano triggering, stress transfer, eruption, earthquake, magma system.

INTRODUCTION

Historical records contain numerous incidences of unusual and explosive volcanism following large earthquakes (Hill et al., 2002; Linde and Sacks, 1998; Marzocchi, 2002). Charles Darwin (1840) described volcanoes in Chile that began erupting after an earthquake in 1835. The Plinian eruption of Santa Maria volcano in Guatemala followed a M 8.3 subduction earthquake in 1902 (Rockstroh, 1903). Hawaii's Mauna Loa erupted repeatedly after volcano-spreading earthquakes (Walter and Amelung, 2006), and eruptions of Vesuvius in Italy are related to earthquakes in the southern Apennines (Nostro et al., 1998). Understanding how earthquakes trigger volcanic activity is important for the interpretation of eruption precursors and for volcano risk mitigation.

An earthquake may increase volcanic activity by dynamic and by static deformation (Hill et al., 2002). Dynamic deformation is transient and caused by seismic body and surface waves, whereas static deformation is permanent and caused by the displacement across a fault and by subsequent viscoelastic relaxation of the crust. Volcanoes 750 km or more from the earthquake epicenters show a statistically significant response immediately after the earthquake (Linde and Sacks, 1998), which indicates that they are triggered by dynamic deformation (Brodsky et al., 1998; Manga and Brodsky, 2006). The effect of static deformation for volcano triggering remains poorly understood, because the type of deformation (contraction or expansion) that is most effective in promoting eruptions is unclear (Marzocchi et al., 2002; Selva et al., 2004). The amplitude of static deformation decays more rapidly with distance from the earthquake than the seismic waves (Hill et al., 2002), thus eruption triggering by static deformation is most likely to be observed at volcanoes located in proximity to an earthquake rupture plane. We study earthquakes at subduction zones with rupture lengths of several hundred kilometers, because they affect a large number of potentially active volcanoes, i.e., the 1952 Kamchatka M 9.0, the 1960 Chile M 9.5, the 1964 Alaska M 9.2, and the 2004 Sumatra-Andaman M 9.3 earthquakes (Fig. 1).

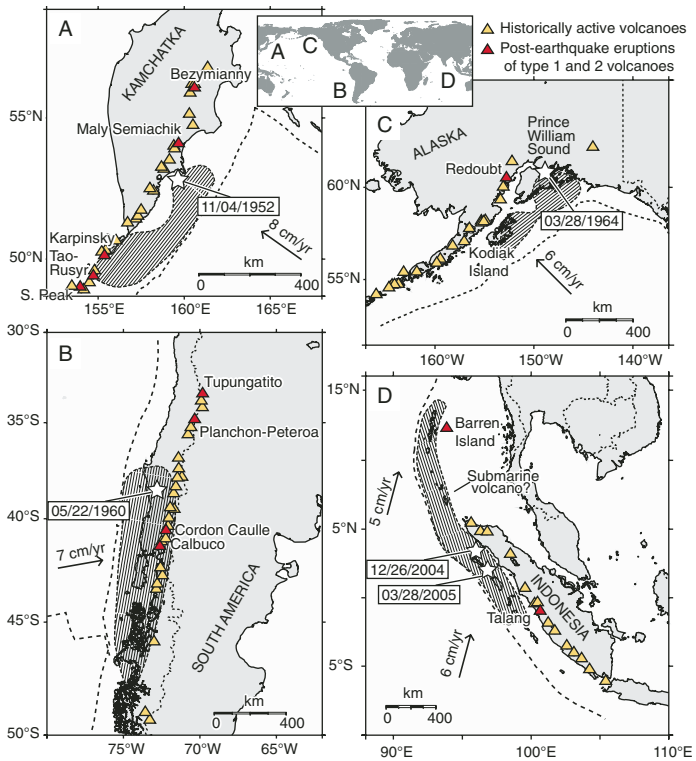

Figure 1. Largest historic earthquakes together with historically active volcanoes: A: Kamchatka M 9.0. B: Chile M 9.5. C: Alaska M 9.2. D: Sumatra-Andaman M 9.3. Earthquake epicenters are given by white star; rupture zone (yellowish shaded area) is based on aftershock distributions and studies by Banerjee et al. (2005), Barrientos and Ward (1990), Holdahl and Sauber (1994), Johnson and Satake (1999), and Yagi (2005). Volcanoes shown by orange triangles; labeled volcanoes erupted within 3 yr after earthquakes are shown by red triangles.

DATA ANALYSIS

Historic Records of Volcanism Following M ≥ 9 Megathrust Earthquakes

To investigate changes in the volcanic activity associated with the earthquakes, we use the 1900–present Global Volcanism Program eruption catalogue (Siebert and Simkin, 2002). In order to reduce unwanted bias in the catalogue, we remove unconfirmed eruptions and eruptions that have uncertainties in time (year and month) and place. We also decluster the catalogue by considering eruptions at the same volcano within six months as one eruption. This leaves us with ~50% of the entire catalogue, out of which we consider volcanoes as much as 1500 km from the earthquake epicenters. To better detect changes above background eruption rate, we classify the volcanoes according to their eruption frequency during the 50 yr prior to the earthquakes. We distinguish volcanoes that had no eruption during this time period (type 1 volcanoes), from volcanoes that erupted rarely (1–4 eruptions, type 2) and intermittently (5–14 eruptions, type 3). We removed semicontinuously erupting volcanoes (with 15 or more eruptions) from the following analysis. We focus hereafter mainly on eruptions at type 1 and type 2 volcanoes, because they are most significant in terms of whether they were triggered by the earthquake, and because most violent historic eruptions (Volcano Explosivity Index [VEI] > 5) occurred at volcanoes that had long periods of quiescence (Marzocchi, 2002; Marzocchi et al., 2002).

Kamchatka 1952 (M 9.0)

The volcanoes of Kamchatka and the Kurile Islands relate to the subduction of the Pacific plate under the Eurasian plate (Fig. 1A) and are ~200 km from the trench. They are among the most active and explosive volcanoes in the world, with more than 450 eruptions since 1900 (Siebert and Simkin, 2002). On 4 November 1952, a 600–700-km-long section of the subduction fault ruptured and caused a M 9.0 earthquake; peak slip exceeded 10 m (Johnson and Satake, 1999). One day later, an eruption occurred at Karpinsky volcano (Fig. 1A). One week later, the Tao-Rusyr Caldera erupted explosively. These were the first ever reported eruptions for both volcanoes (type 1 volcanoes). On 5 December 1952, an eruption occurred at Maly Semiachik volcano (type 2), and in August 1954 at Sarychev Peak (type 2). Tolbachik (type 3) erupted in 1954 and twice in 1955. In October 1955, a flank collapse triggered the first historic eruption of Bezymianny (type 1), which has been continuously active ever since.

Chile 1960 (M 9.5)

The subduction of the Nazca plate under the South American plate is associated with a line of active volcanoes ~250 km from the trench (Fig. 1B). The great M 9.5 Chile earthquake of 22 May 1960 resulted from rupture of an ~900-km-long portion of the plate boundary (Cifuentes and Silver, 1989), with a mean slip of ~17 m and peak slip of as much as 40 m (Barrientos and Ward, 1990). Just two days after the earthquake, Cordón-Caulle volcano, located near the earthquake epicenter, had its first eruption in 16 yr (type 2). The volcanoes Planchón-Peteroa and Tupungatito both erupted once in July 1960 and again in 1961–1962 (type 2). Calbucu volcano erupted 8 months after the earthquake, which was its first eruption for 32 yr (type 2), followed by the eruption at Villarrica volcano (type 3) in February 1963.

Alaska 1964 (M 9.2)

Most of the active volcanoes are located in the Aleutian Islands at a distance of 150 km from the trench (Fig. 1C). This distance and the spacing between the volcanoes increase toward the east of the Alaska Peninsula. The M 9.2 Alaska earthquake of 28 March 1964 resulted from rupture of an 800-km-long portion of the subduction fault, with peak slip of ~30 m (Holdahl and Sauber, 1994). In May 1964, Trident volcano erupted (type 3). In January 1965, 10 months after the earthquake, unusually strong degassing was reported at Redoubt volcano, and was followed by eruptions in January 1966 and October 1966. These were the first eruptions at Redoubt after 64 yr of quiescence (type 1 volcano).

Sumatra-Andaman 2004–2005 (M 9.3 and M 8.7)

The subduction of the Indo-Australian plate under the Sunda plate results in a line of subaerial volcanoes on Sumatra and the Andaman Islands, and submarine volcanoes in between (Fig. 1D). On 26 December 2004 a subduction zone rupture initiated near the coast of northern Sumatra, and progressively extended northward, unzipping more than 1200 km of the plate boundary with maximum slip of as much as 15 m (Ammon et al., 2005). The resultant M 9.3 earthquake transferred stress southward, where an M 8.7 earthquake occurred on 28 March 2005 (Ammon et al., 2005; McCloskey et al., 2005). Aftershocks migrated farther south, to where the volcano Talang (type 2) erupted on 10 April 2005 only 12 days after the second Sumatra earthquake. Barren Island (type 2) then began erupting on 28 May 2005. In addition, during the last week of January 2005, a seismic swarm with more than a hundred M > 5 earthquakes occurred east of the Nicobar Islands, possibly indicating submarine volcanic activity (see GSA Data Repository Section 1[1]).

Statistical Tests of Eruption Rate Changes

To test whether the earthquakes changed the eruption rate we consider only volcanoes in the vicinity of the earthquake rupture. We define vicinity as the area of earthquake-induced volumetric expansion (see following). We compare average eruption rates (AER) during a 50 yr period before the earthquake with postearthquake eruption rates (PER) during a 3 yr time period following the earthquake. In total, in the 50 yr before the Kamchatka, Chile, and Alaska earthquakes, no type 1 volcano erupted (AER = 0), whereas within the 3 yr after the earthquakes, 5 type 1 eruptions occurred (PER = 1.7). For type 2 and type 3 volcanoes, the PERs are about twice the AERs. The differences between AERs and PERs are also significant for the individual subduction zones. For type 1 and type 2 volcanoes, the AERs and PERs range from 0.1 to 0.6 and from 2.9 to 8.3 eruptions per year, respectively (see GSA Data Repository Section 3). In other words, on average <1 eruption occurred per year prior to the earthquake, whereas there were 3–8 eruptions within the 3 yr after the earthquake. One year after the earthquake, the PER for type 1 and 2 volcanoes in Sumatra-Andaman is already almost 4 times the AER. The rate increases are largest for volcanoes that had no eruptions prior to the earthquakes (type 1 volcanoes). Although caution is required when conclusions are drawn from data populations with small numbers, the sudden increase of eruptions of previously quiet volcanoes (type 1) during the 3 yr postearthquake period makes us confident that the correlation is real. Additional tests are presented in the GSA Data Repository Section 3, all showing that the increase in volcanic activity is significant.

Boundary Element Models of Earthquake Deformation

Subduction zones consist of a seismic zone at a depth interval of ~10–50 km, enclosed by an aseismic zone. Most of the time, the seismic zone is partly locked and accumulates stress. During an earthquake, the accumulated stress is released as the overriding plate slips seaward over the subducting plate. To test whether eruptions may be related to such earthquakes, we examine the volumetric strain Δ, which is the sum of the normal components of the strain tensor. By convention, negative volumetric strain corresponds to volumetric contraction (compressing the rock), and positive volumetric strain corresponds to volumetric expansion (decompressing the rock). A subduction earthquake is associated with volumetric contraction in the near-trench portion of the forearc and volumetric expansion in the far-trench portion, possibly at the volcanoes (Fig. 2).

The calculations are performed in a three-dimensional linear elastic medium, using a modified version of Poly3D, a boundary element model

[1]GSA Data Repository item 2007125, DR Sections 1, 2, and 3, is available online at www.geosociety.org/pubs/ft2007.htm, or on request from editing@geosociety.org or Documents Secretary, GSA, P.O. Box 9140, Boulder, CO 80301, USA.

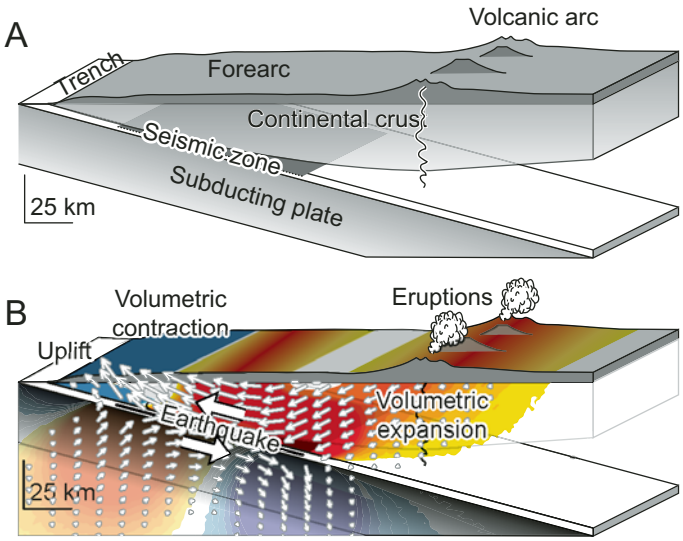

Figure 2. A: Schematic cross sections of subduction zone. B: Displacement field (arrows) and volumetric deformation (red colors for volumetric expansion, blue colors for volumetric contraction) associated with megathrust earthquake. Volcanic system undergoes volumetric expansion by earthquake.

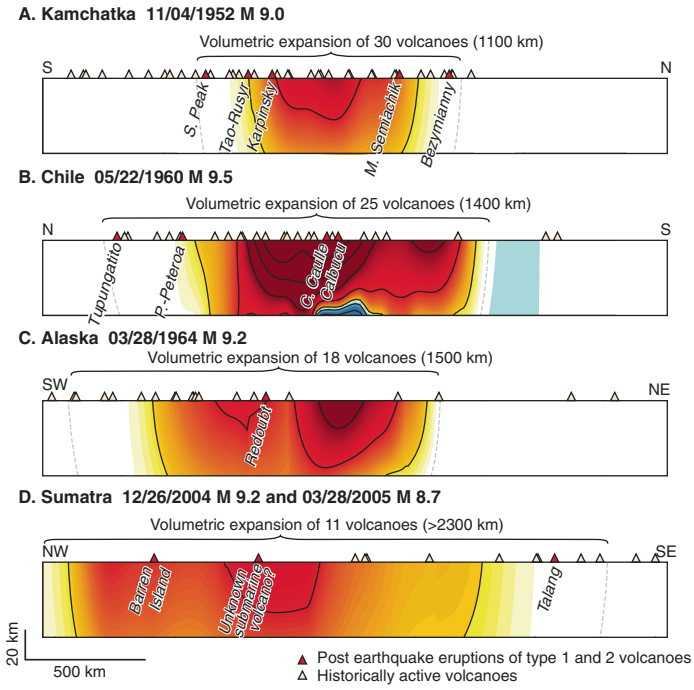

Figure 3. Volumetric deformation associated with megathrust earthquakes in cross sections along volcanic lines of (A) Kamchatka, (B) Chile, (C) Alaska, and (D) Sumatra-Andaman together with historically active volcanoes (orange triangles) and volcanoes that erupted during 3 yr following earthquakes (red triangles). Red colors indicate positive strain (volumetric expansion), blue colors indicate negative strain (volumetric contraction). Contours represent 0 μ strain (dashed line) and 5 μ strain increments (solid black lines).

code based on the analytical solutions for triangular dislocations in isotropic half-spaces and full spaces (Thomas, 1993). To calculate deformation at the line of active volcanoes, we define vertical observation planes that follow the coordinates of the historically active volcanoes for a length of 3000 km, with a depth from 0 to 50 km. Grid spacing is 2 km. We assume a Poisson's ratio of $\nu = 0.25$ and Young's Modulus of $E = 50$ GPa. The effect of the plate curvature were neglected because the input parameters derive from published half-space inversions and because the volcanic lines are generally <200 km from the earthquake, so the effect is of minor importance. The model geometry and further details are given in the GSA Data Repository Section 2.

Elastic numerical modeling of the Kamchatka, Chile, Alaska, and Sumatra-Andaman earthquakes with published slip distributions shows that in all cases the volcanic lines underwent volumetric expansion (red in Figs. 3A–3D). The modeling results are shown in cross sections from the surface to a depth of 50 km along the lines of active volcanoes. For each earthquake, the along-strike area of expansion is longer than the fault length, extending as much as 2300 km for the Sumatra-Andaman earthquake. Volumetric expansion is strongest for the Chile earthquake, with up to 28 μ strain near the subsequently active Cordon Caulle and Calbucu volcanoes (Fig. 3B; see also Barrientos, 1994). Volumetric contraction in the along-strike direction for the Chile earthquake is the result of the oblique convergence, and for the Alaska earthquake is related to the bend in the subduction zone (blue in Figs. 3B, 3C).

Figure 3 also shows the volcanoes that erupted in the first 3 yr after the earthquakes. The principal observation is that all the erupted type 1 and 2 volcanoes underwent volumetric expansion induced by the earthquake. Also, with the exceptions of Pavlof and Shishaldin in Alaska, which are >1000 km from the earthquake and so are probably not related to coseismic static deformation, the type 3 eruptions occurred within the dilatational area as well.

SUMMARY AND DISCUSSION

Eruption triggering depends on the initial state of the magmatic system prior to the earthquake, i.e., on magma composition, state of equilibrium of magma and volatiles, magma overpressure, and the strength of the host rocks, and on the type, size, and distance of the earthquake (Hill et al., 2002). Due to such inherent complexity in magmatic systems and associated feedbacks, triggered eruptions therefore may occur with a delay of days, months, or years after an earthquake.

Different types of stress changes are currently discussed, where dynamic stresses associated with seismic waves are large in magnitude but not permanent, whereas static changes are smaller but permanent (Manga and Brodsky, 2006). Our study suggests that the eruption rate increases in the region of permanent expansion. This implies that permanent deformation, besides dynamic shaking (Manga and Brodsky, 2006), has an important effect for volcano triggering. However, it may appear as a counterintuitive conclusion that volume expansion leads to a pressure increase within a magmatic system. The interplay of silicate melts and gases following coseismic depressurization may be the key to increase the magma overpressure and eventually lead to an eruption (Fig. 4).

The dissolved volatile gases CO_2 and H_2O influence the density and viscosity of host magmas, and play a crucial role for eruption triggering. Mechanisms to generate magma overpressure include (1) the intrusion and mixing of compositionally dissimilar magmas (Sparks

How earthquakes may trigger eruptions

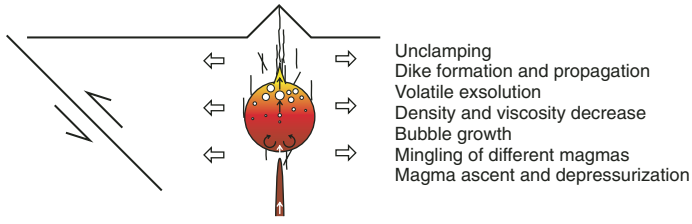

Figure 4. Sketch summarizing triggering mechanisms by earthquake deformation.

et al., 1977) that may release large amounts of exsolved gases into the reservoir and cause volumetric expansion (Eichelberger, 1980), and (2) the nucleation, growth, and ascent of volatile phases through shaking (Manga and Brodsky, 2006). There may be a positive feedback loop that eventually leads to an eruption. Volumetric expansion or ascent of basaltic magma leads to the exsolution of CO_2, which decreases the magma density and viscosity, which enhances the ascent of gas bubbles and of the magma, which causes additional depressurization, further volatile exsolution, and volume expansion of the gas. Exsolution of water may stop this process, as it causes the viscosity of the ascending magma to increase (Dixon et al., 1995), resulting in magma stagnation. This is more likely to be the case for H_2O- rich silicic magmas (Dixon et al., 1995). In some cases it was suggested that postearthquake eruptions were triggered by basaltic magma ascent and mixing with other magma reservoirs (Eichelberger, 1980).

Earthquakes can influence not only the timing but also the structural mechanism of eruptions. An excellent example for this is the 1960 eruption of Cordón Caulle volcano two days after the Chile earthquake. The eruptive fissure was fed by a dike oriented normal to the direction of the earthquake slip (Sepulveda et al., 2005). The Chile earthquake induced ~30 μ strain at the volcanic system of Cordon Gaulle volcano (a 1 km section of the rock mass was dilated by 3 cm in all directions). This expansion together with an unclamping of the fracture system may have encouraged the dike to intrude in the NW direction.

If our hypothesis, that earthquake-induced volumetric expansion causes an increase of the magma-gas pressure and so encourages eruptions, is correct, then corresponding volumetric contraction may decrease the gas pressure and discourage eruptions. A similar understanding is also applied in seismology, where the earthquake-induced deformation field provides an accurate guide to which faults are brought closer to and further away from rupturing (Stein, 1999).

Our study suggests that postseismic eruptions occur mainly at type 1 and type 2 volcanoes located within the dilatational area, implying (1) that rarely erupting volcanoes are more susceptible to extrinsic triggering, and (2) that expansion has a large influence on eruption potential. These results have important general and specific implications for volcano hazard estimation following earthquakes. Through our analysis we can now estimate which volcanoes are brought closer to eruption as a function of the static deformation field induced by earthquake rupture. For the Sumatra-Andaman arc, we can predict or may expect new eruptions in the next few years at volcanoes that hitherto have shown little or no activity in the recent past and would otherwise be regarded as low-risk volcanoes by current methods of evolution.

ACKNOWLEDGMENTS

We thank L. Siebert and T. Simkin for providing the updated global volcano eruption database. The program Poly3d was provided by D. Pollard, Stanford University. Walter was supported by the Emmy Noether Junior Research Program of the German Research Council (DFG WA 1642/1-4) and Amelung was supported by the National Science Foundation (EAR Geophysics program).

REFERENCES CITED

Ammon, C.J., Ji, C., Thio, H.K., Robinson, D., Ni, S., Hjorleifsdottir, V., Kanamori, H., Lay, T., Das, S., Helmberger, D., Ichinose, G., Polet, J., and Wald, D., 2005, Rupture process of the 2004 Sumatra-Andaman earthquake: Science, v. 308, p. 1133–1139, doi: 10.1126/science.1112260.

Banerjee, P., Pollitz, F.F., and Burgmann, R., 2005, Geophysics: The size and duration of the Sumatra-Andaman earthquake from far-field static offsets: Science, v. 308, p. 1769–1772, doi: 10.1126/science.1113746.

Barrientos, S.E., 1994, Large thrust earthquakes and volcanic eruptions: Pure and Applied Geophysics, v. 142, p. 225–237.

Barrientos, S.E., and Ward, S.N., 1990, The 1960 Chile earthquake; inversion for slip distribution from surface deformation: Geophysical Journal International, v. 103, p. 589–598.

Brodsky, E.E., Sturtevant, B., and Kanamori, H., 1998, Earthquakes, volcanoes, and rectified diffusion: Journal of Geophysical Research, v. 103, p. 23,827–23,838, doi: 10.1029/98JB02130.

Cifuentes, I.L., and Silver, P.G., 1989, Low-frequency source characteristics of the great 1960 Chilean earthquake: Journal of Geophysical Research, v. 94, p. 643–663.

Darwin, C., 1840, On the connexion of certain volcanic phenomena in South America; and on the formation of mountain chains and volcanos, as the effect of the same power by which continents are elevated: Geological Society [London] Transactions, v. 2, p. 601–632.

Dixon, J.E., Stolper, E.M., and Holloway, J.R., 1995, An experimental study of water and carbon dioxide solubilities in mid-ocean ridge basaltic liquids; Part I, Calibration and solubility models: Journal of Petrology, v. 36, p. 1607–1631.

Eichelberger, J.C., 1980, Vesiculation of mafic magma during replenishment of silicic magma reservoirs: Nature, v. 288, p. 446–450, doi: 10.1038/288446a0.

Hill, D.P., Pollitz, F., and Newhall, C., 2002, Earthquake-volcano interactions: Physics Today, v. 55, p. 41–47.

Holdahl, S.R., and Sauber, J., 1994, Coseismic slip in the 1964 Prince William Sound earthquake: A new geodetic inversion: Pure and Applied Geophysics, v. 142, p. 55–82, doi: 10.1007/BF00875968.

Johnson, J.M., and Satake, K., 1999, Asperity distribution of the 1952 great Kamchatka earthquake and its relation to future earthquake potential in Kamchatka: Pure and Applied Geophysics, v. 154, p. 541–553, doi: 10.1007/s000240050243.

Linde, A.T., and Sacks, I.S., 1998, Triggering of volcanic eruptions: Nature, v. 395, p. 888–890, doi: 10.1038/27650.

Manga, M., and Brodsky, E.E., 2006, Seismic triggering of eruptions in the far field: Volcanoes and geysers: Annual Review of Earth and Planetary Sciences, v. 34, p. 263–291, doi: 10.1146/annurev.earth.34.031405.125125.

Marzocchi, W., 2002, Remote seismic influence on large explosive eruptions: Journal of Geophysical Research, v. 107, p. 6-1–6-7.

Marzocchi, W., Casarotti, E., and Piersanti, A., 2002, Modeling the stress variations induced by great earthquakes on the largest volcanic eruptions of the 20th century: Journal of Geophysical Research, v. 107, B11 2320, doi: 10.1029/2001JB001391.

McCloskey, J., Nalbant, S., and Steacy, S., 2005, Earthquake risk from co-seismic stress—Last year's Indonesian earthquake has increased seismic hazard in the region: Nature, v. 434, p. 291, doi: 10.1038/434291a.

Nostro, C., Stein, R.S., Cocco, M., Belardinelli, M.E., and Marzocchi, W., 1998, Two-way coupling between Vesuvius eruptions and southern Apennine earthquakes, Italy, by elastic stress transfer: Journal of Geophysical Research, v. 103, p. 24,487–24,504, doi: 10.1029/98JB00902.

Rockstroh, E., 1903, Recent earthquakes in Guatemala: London, Nature, v. 66, p. 150.

Selva, J., Marzocchi, W., Zencher, F., Casarotti, E., Piersanti, A., and Boschi, E., 2004, A forward test for interaction between remote earthquakes and volcanic eruptions: The case of Sumatra (June 2000) and Denali (November 2002) earthquakes: Earth and Planetary Science Letters, v. 226, p. 383–395, doi: 10.1016/j.epsl.2004.08.006.

Sepulveda, F., Lahsen, A., Bonvalot, S., Cembrano, J., Alvarado, A., and Letelier, P., 2005, Morpho-structural evolution of the Cordón Caulle geothermal region, Southern Volcanic Zone, Chile: Insights from gravity and 40Ar/39Ar dating: Journal of Volcanology and Geothermal Research, v. 148, p. 207–233,

Siebert, L., and Simkin, T., 2002, Volcanoes of the world: An illustrated catalog of Holocene volcanoes and their eruptions: Smithsonian Institution Global Volcanism Program Digital Information Series GVP-3.

Sparks, R.S.J., Sigurdsson, H., and Wilson, L., 1977, Magma mixing; a mechanism for triggering acid explosive eruptions: Nature, v. 267, p. 315–318, doi: 10.1038/267315a0.

Stein, R.S., 1999, The role of stress transfer in earthquake occurrence: Nature, v. 402, p. 605–609, doi: 10.1038/45144.

Thomas, A.L., 1993, Poly3D: A three-dimensional, polygonal element, displacement discontinuity boundary element computer program with applications to fractures, faults, and cavities in the earth's crust [M.S. thesis]: Stanford, California, Stanford University, 221 p.

Walter, T.R., and Amelung, F., 2006, Volcano-earthquake interaction at Mauna Loa Volcano, Hawaii: Journal of Geophysical Research, v. 111, B05204, doi:10.1029/2005JB003861.

Yagi, Y., 2005, Preliminary results of rupture process for 2004 off coast of northern Sumatra giant earthquake, ver. 1: http://iisee.kenken.go.jp/staff/yagi/eq/Sumatra2004/Sumatra2004.html (January 2007).

Manuscript received 18 October 2006
Revised manuscript received 19 January 2007
Manuscript accepted 25 January 2007

Printed in USA